Invited Paper

Scanning micromirrors: An overview

P. R. Patterson[a], D. Hah[b], M. Fujino[c], W. Piyawattanametha[b], and M.C. Wu[b]
[a]HRL Laboratories, LLC, 3011 Malibu Canyon Road, Malibu, CA 90265
[b]Electrical Engineering Department, University of California, Los Angeles
Room 63-128, Eng. IV Building, 405 Hilgard Ave., Los Angeles, CA 90095
[c]TOPCON CORP., R&D Center, 75-1, Hasunuma-cho, Itabashi-ku,
Tokyo, 174-8580, Japan

ABSTRACT

An overview of the current state of the art in scanning micromirror technology for switching, imaging, and beam steering applications is presented. The requirements that drive the design and fabrication technology are covered. Electrostatic, electromagnetic, and magnetic actuation techniques are discussed as well as the motivation toward combdrive configurations from parallel plate configurations for large diameter (mm range) scanners. Suitability of surface micromachining, bulk micromachining, and silicon on insulator (SOI) micromachining technology is presented in the context of the length scale and performance for given scanner applications.

Keywords: Scanning micromirror, MEMS, optical switching, MOEMS, vertical combdrive

1. INTRODUCTION

Micro-electro-mechanical systems (MEMS) technology enables the creation of micro-optical elements which are inherently suited to cost effective manufacturability and scalability as the processes are derived from the very mature semiconductor microfabrication industry. The inherent advantages of applying microelectronics technology to silicon micromechanical devices including optical MEMS were presented in 1982 by Petersen in the now classic paper, “Silicon as a Mechanical Material”.[1] The ability to steer or direct light is a key requirement for free space optical systems and in the 22 years since Petersen’s silicon scanner[2], the field of optical MEMS has seen explosive growth.[3,4]

The rapid development of optical MEMS is a direct result of market driven applications. In the 80’s and early 90’s, displays were the main driving force for the development of micromirror arrays. Portable digital displays are commonplace (the same technology is now available in large screen televisions) and head-mounted retinal scanning displays, while not as prevalent, are commercially available. In the past decade, telecommunications have become the market driver for optical MEMS. The demand for routing ever increasing internet traffic through fiber optic networks pushed the development of both digital and scanning micromirror systems for large port count all optical switches; indeed the switching capacity realized by scanning micromirror arrays has outpaced current demand.[5] In the healthcare arena, scanning optical devices promise low cost, endoscopic, optical cross-sectioning systems for *in vivo* diagnostics. MEMS micromirrors are candidates for virtually any application where miniaturization, lightweight, low energy consumption, and/or reduced cost provide the incentive to replace existing macromirrors. Such a broad range of applications requires many types of MEMS micromirrors, from the small (~200 μm) component micromirrors in large arrays to the very large (several to tens of mm) scanners in high resolution imaging systems.

2. REQUIREMENTS FOR SCANNING MICROMIRRORS

Generally speaking, performance of a scanning micromirror is determined by the maximum scan angle, resonant frequency, resolution, and surface quality with respect to flatness and smoothness. The preferred microfabrication technology as well as the performance is closely linked to the size of the micromirror and therefore length scale is a convenient way to classify MEMS scanners. A summary of the applications and main fabrication technologies of various

Optomechatronic Micro/Nano Components, Devices, and Systems, edited by Yoshitada Katagiri,
Proc. of SPIE Vol. 5604 (SPIE, Bellingham, WA, 2004) · 0277-786X/04/$15 · doi: 10.1117/12.582849

micromirror devices with length scale ranging from micrometers to millimeters is shown in Fig.1. High-resolution imaging applications require large mirrors and large scan angles. Resolution as defined by the number of resolvable spots is a function of the beam divergence and the scan range (Fig. 2) as shown in the following equations:

$$N = \frac{\theta_{max}}{\delta\theta} = \frac{\theta_{max} D}{a\lambda} \tag{1}$$

Where: $\delta\theta$ is beam divergence, θ_{max} is the total optical scan range, D is the mirror diameter, λ is the wavelength of incident light, and *a* is the aperture shape factor (*a*=1 for a square aperture and 1.22 for a circular aperture[6]).

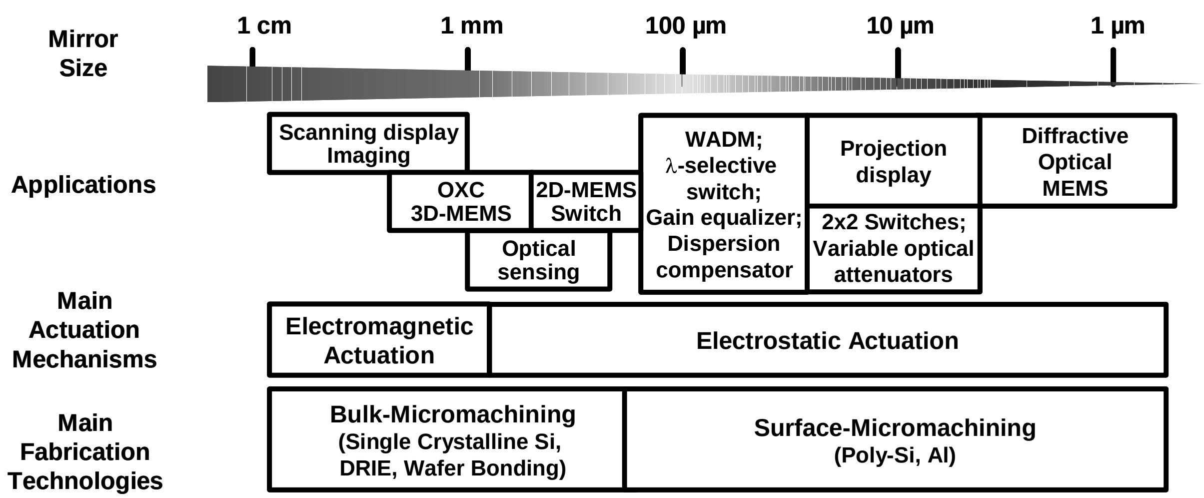

Fig.1 Applications and fabrication technologies for micromirror devices with length scale ranging from micrometers to millimeters.[7]

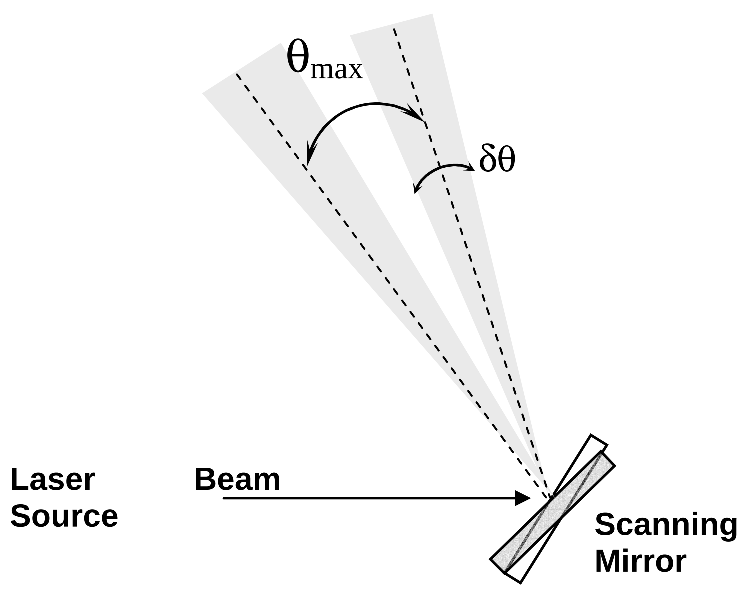

Fig. 2 Simplified diagram showing reference for maximum scan angle and beam divergence for scanning micromirror.

Imaging or display applications involving raster scanning, require a dual axis system with fast scanning capability. This may be accomplished by combining two 1-D scanners [8] or by a single biaxial scanner typically designed with a gimbal structure. The maximum scan speed is dictated by the resonant frequency which is in turn determined by the mechanical properties of the scanner, specifically the mass and spring constant.

The natural frequency for torsional displacement is given by:

$$\omega_0 = 2\pi f_0 = \sqrt{\frac{k}{I}} \tag{2}$$

For a square mirror,

$$I = \frac{1}{12} mL^2 \tag{3}$$

Where: I is the mass moment of inertia, k is the spring constant, L is the diameter of mirror, ω_0 is the natural frequency, and m is the mass of the mirror.

Very large area mirrors with a length scale > 2 mm benefit from electromagnetic actuation since the Lorentz force is proportional to the mirror area. To maintain the flatness of large mirrors, such devices are typically fabricated in single crystal silicon (SCS) derived from a bulk substrate or silicon on insulator (SOI). In the 250 μm to 1 mm range, electrostatic actuation is more advantageous and current trends favor higher force electrostatic combdrives over parallel plate type actuators, and SOI MEMS over surface micromachining. For micromirror devices below 250 μm, surface micromachining offers higher integration and multi-level interconnect, features which are ideal for large mirror arrays consisting of small component scanners. In this review we will focus on large area scanners.

3. ELECTROSTATIC SCANNERS

Electrostatic micromirrors with torsional rotation can be described as follows: when voltage is applied between the movable and the fixed electrodes, the mirror rotates about the torsion axis until the restoring torque and the electrostatic torque are equal. The torques can be expressed as:

$$T_e(\theta) = \frac{V^2}{2}\frac{\partial C}{\partial \theta} \tag{4}$$

$$T_r(\theta) = k\theta \tag{5}$$

Where V is the applied voltage, C is the capacitance of the actuator, θ is the rotation angle, and k is the spring constant.

The capacitance is determined by the area of the electrode overlap and the gap between the electrodes. For simple parallel plate geometry, the capacitance can be expressed by

$$C = \frac{\varepsilon_0 A}{g} \tag{7}$$

Where ε_0 is the permittivity of free space, A is the area of electrode overlap, and g is the gap between fixed and moving electrodes.

Electrostatic actuation is currently the predominant method used for MEMS scanners. There are two main configurations for electrostatic scanning micromirrors: parallel plate and vertical combdrive, (Fig. 3). For the parallel-plate type mirror, the area of the electrode overlap is essentially the area of the fixed electrode and the gap is a function of the rotation angle; here there is a tradeoff as the initial gap spacing needs to be large enough to accommodate the scan angle, but small enough for reasonable actuation voltage. This is further exacerbated by a pull-in phenomenon which renders 60-66% of the gap spacing unstable.[9,10] The vertical combdrive offers an improved situation, the mirror and the actuator are decoupled, and the gap between the interdigitated fingers of the combdrive is typically quite small on the order of several microns. In the combdrive, the gap is constant and the area of the electrode overlap is a function of the rotation angle.

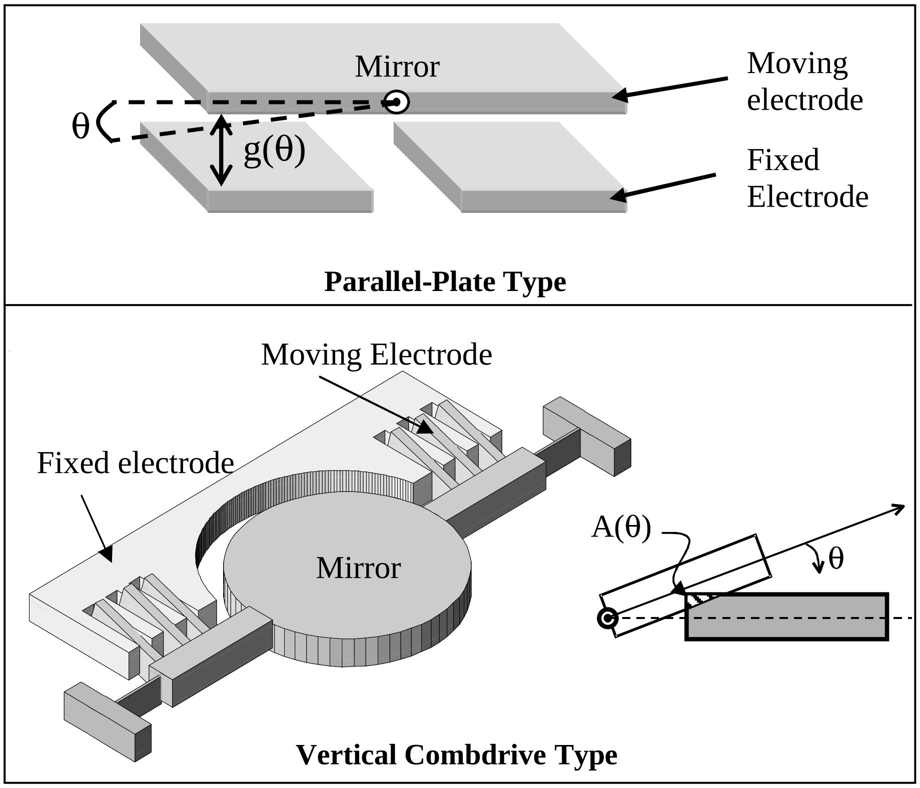

Fig. 3 Perspective view of parallel-plate type (Top) and vertical combdrive type (Bottom) electrostatic micromirrors.

3.1 Electrostatic Parallel-Plate Scanners

Parallel-plate type scanners can be realized by using either surface or bulk micromachining technologies, or a combination of both. Surface-micromachined scanners can be fabricated with a standard foundry process, such as the Multi-User MEMS Process (MUMPs).[11] However, assembly is required to raise the mirror above the substrate. Fan and Wu [12] have reported a 400 x 400 μm^2 parallel-plate scanner. The polysilicon mirror is lifted-up vertically to 200 μm above substrate using a microactuated 3-D structure called micro-elevator by self-assembly (MESA).[13] Lucent technologies employed a self-assembly technique which was driven by the residual stress in deposited thin films (Cr/Au on polysilicon) to raise two-axis polysilicon scanners (500 μm mirror diameter) to a fixed position 50 μm above the substrate.[14,15] Two-axis scanning is achieved by electrostatic force between the mirror and the quadrant electrodes on the substrate. Fan's scanner has a static optical scan range of 28° and a drive voltage of 70 V. Resonant frequency for the mirror was measured at 1.5 kHz.

Telecommunication has been the main driver for the 2-axis scanner to enable large port count switches. In dense wavelength-division-multiplexed (DWDM) networks, there is a need for optical crossconnect (OXC) with large port count. [16,17,18] The dual axis analog scanning capability is key for these applications since each mirror associated with the input fiber array can point to any mirror associated with the output fiber array (Fig. 4). This allows for N^2 optical interconnects with 2N component mirrors, and therefore a configuration scalable to very large port count switches. This configuration is often referred to as a 3-D MEMS switch because the optical beams propagate in three-dimensional space. Square mirror arrays with up to 256 scanning micromirrors have been demonstrated with a surface micromachined process for OXC applications.[16,19,20]

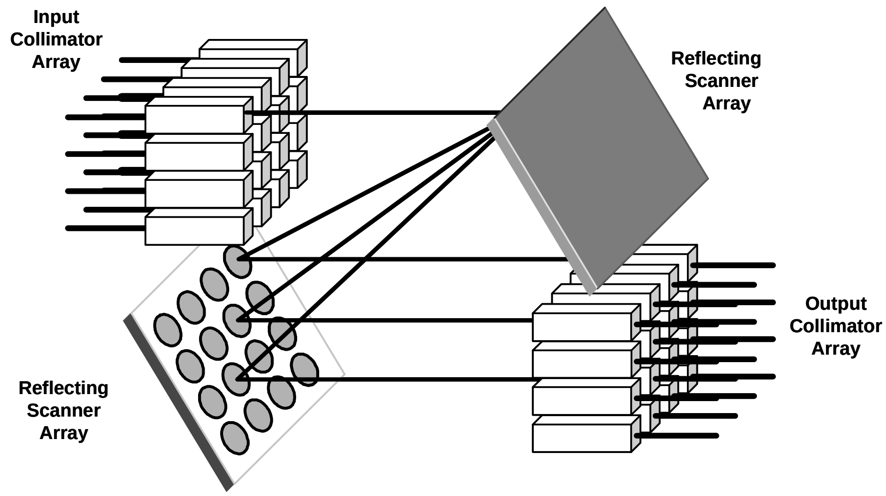

Fig. 4 Configuration for 3-D optical switch for N input fibers and N output fibers (NxN) and which requires 2N analog scanning mirrors (after Lin and Goldstein [17])

The port count of a 3-D MEMS switch is limited by the size and flatness of the micromirrors, as well as their scan angle and fill factor. For a complete discussion of scaling laws for MEMS free space optical switches see Syms[18]. For large port count (approaching 1000 x 1000), single crystal micromirror scanners are necessary to achieve large mirror size with required flatness. Micromirrors fabricated by standard polysilicon surface-micromachining processes can have significant curvature due to residual stress and stress gradient of the deposited thin films. Even for flat mirrors with balanced stress, the difference of thermal expansion coefficients between the thin mirror and the metal coating causes the mirror curvature to change with temperature. Techniques to improve the curvature of polysilicon micromirrors have been reported: by incorporating an outer edge folded frame in the mirror film formed by depositing the polysilicon in an etched trench [21]; by exploiting the tensile stress of the polysilicon to create a drum like mirror structure on a rigid solid frame [22]; and by a combination of high temperature annealing and thick polysilicon cross bar support structures.[23]

Hybrid structures that utilize single crystal silicon for the mirror structure and polysilicon for the actuators offer an alternative to polysilicon mirrors. Su et al., showed that the mirror curvature improved by 150 times (from 1.8 cm to 265 cm) by bonding a 22.5-μm-thick SCS mirror to a surface-micromachined actuator. [24,25] Scanners with 1-mm SCS honeycomb micromirrors created by deep reactive ion etching (DRIE) and silicon fusion bonding have also been reported for reducing the mirror weight and increasing resonant frequency.[26] Hybrid devices have also been demonstrated with a fluidic self-assembly technique utilizing low temperature adhesives and selective surface treatments of the polysilicon receptor and a thin (15 μm) SCS mirror.[27] Gold compression bonding of two different surface micromachined MUMPS chips has been used to increase the number of layers and the design flexibility for mirror arrays. [28,29]

A clear trend for electrostatic scanning micromirrors with mirror size in the 0.5 -1 mm size range is toward the use of SOI-MEMS and simplified fabrication methods.[30] The materials and concept are identical to the first reported MEMS scanner [2], but with the current state of the art applied. An example is the 2-axis scanner reported by Analog Devices.[31] The scanner is realized using a three-layer approach. The top two layers are from an SOI wafer with a 10-μm-thick device layer. The top layer is used for mirrors and mechanical springs, as well as integrated control electronics. After backside etching, the wafer is bonded to a bottom wafer with polysilicon electrodes for electrostatic actuation and capacitive sense of mirror position. The electrodes are contacted through polysilicon-filled via posts. A similar electrostatic parallel-plate scanner has been recently reported from Corning Intellisense.[32] Corning's mirrors were derived from a single 100 μm SOI which was patterned and etched down to 3-4 μm in areas intended for the torsion flexures, and to 14 μm in areas intended for the mirrors. The SOI was anodically bonded to a glass substrate housing patterned metal electrodes. Arrays containing 320 scanners each at 750 x 800 μm^2 were demonstrated with component mirror mechanical scan range of 10° at 60V. The resonant frequencies for both mirror axes were reported as in the 200-400 Hz range. Using bulk micromachining, NTT has developed a "terraced bottom electrode" to reduced the operating voltage.[33,34] It should be noted that the resonant frequency requirement is relaxed in optical switching applications (compared to imaging applications) since switching times of several milliseconds are acceptable.

Using two chips of 2-axis SCS micromirror arrays, each with 36 x 36 = 1296 elements, Ryf et al. have reported a 1296 port OXC.[35] Light was coupled to the micromirror arrays through a matched 2-D fiber collimator array. The maximum operating voltage of the scanning mirror is 200 V. Connections measured between 60 input ports and 60 output ports exhibited a mean insertion loss of 5.1 dB ± 1.1 dB. Crosstalk during beam scanning was less than – 38 dB, and after the connection was established, the crosstalk to adjacent channels was – 58 dB. The switching time was 5 msec. For OXC's with smaller port count, low loss can be obtained even with surface-micromachined scanning micromirrors. Aksyuk et al. reported a mean insertion loss of 1.33 dB and maximum loss of 2.0 dB for all 56,644 connections in a 238 x 238 switch fabric. [36] The improved performance is attributed to tight control of the MEMS and optical components, including large radius of curvature of mirrors (loss due to mirror curvature < 0.3 dB), low aberration (~ $\lambda/10$) and focal length variation (~ 1%) of microlens arrays, and low position and point error of fibers in the array. The optical path length in the switch fabric has also been minimized. Kim et al. have tested the mechanical stability by switching the mirror over 18 billion cycles in 38 weeks in dry ambient at room temperature. [37] No measurable change in device performance was found. When the switch was operated without invoking feedback control, the loss variation is less than 0.1 dB over 120 hours of testing for a connection with fixed bias on the mirrors.

3.2 Electrostatic Vertical Combdrive Scanners

Electrostatic combdrives are efficient at utilizing the driving voltage due to the narrow gap between the fixed and moving electrodes. The first MEMS electrostatic combdrives, demonstrated by Tang et al.,[38] in 1989 were lateral combdrives formed in polysilicon. For lateral combdrives, the moving comb travels in-plane relative to the fixed comb, parallel to the substrate. Lateral combdrives have been used for scanning micromirrors [39], but vertical combdrives are much more prevalent. In the vertical combdrive, moving comb motion is out of the fixed comb plane and perpendicular to the substrate. The first vertical combdrive was introduced by Selvakumar et al. [40,41] and featured a fixed comb etched in the silicon substrate and a moving comb formed in polysilicon with the entire structure spanning an etch pit in the substrate.

Vertical combdrive actuation offers some key advantages over parallel plate type actuation for electrostatic scanning micromirrors. Decoupling of the mirror and actuator removes the restriction on the maximum deflection (scan angle) imposed by geometry of the parallel plate. In addition, the pull-in associated with the parallel plate can be avoided in the vertical combdrive. (It should be noted that pull-in of a parallel plate scanner can be mitigated by feed back control.[42]) The large electrostatic torque allows for the design of a relatively stiff torsion bar, this increases the resonant frequency and therefore the scan speed and bandwidth of the device. Higher resonant frequencies also provide insurance against unwanted excitation from environmental vibrations. The vertical combdrive requires a disruption of the electrostatic field between the combs for actuation. Devices designed strictly for resonant mode operation require only a slight asymmetry between the fixed and moving areas as demonstrated by Schenk et al.,[43] However, for quasi-static or DC operation, the distance from the top of the moving comb to the top of the fixed comb (in the un-actuated state) determines the range of motion, so the fixed and moving combs are designed in separate planes.

There are several ways to combine vertical combdrive actuation with micromirrors. As shown in Fig. 5, the vertical combs can be integrated (a) underneath the mirror, (b) on a shaft parallel to the torsion bar, or (c) on the edge of the mirror. Alignment of the top and the bottom combs plays a critical role in the performance of the scanner. Misalignment of the combs could lead to lateral instability and limit the scan range. Recent efforts have been focused on the development of self-aligned processes or device structures, as will be discussed below. Another important parameter is the gap spacing between the movable and the fixed combs. The electrostatic torque is inversely proportional to the gap spacing. The minimum spacing will be determined by the comb alignment and the aspect ratio of the etched comb fingers.

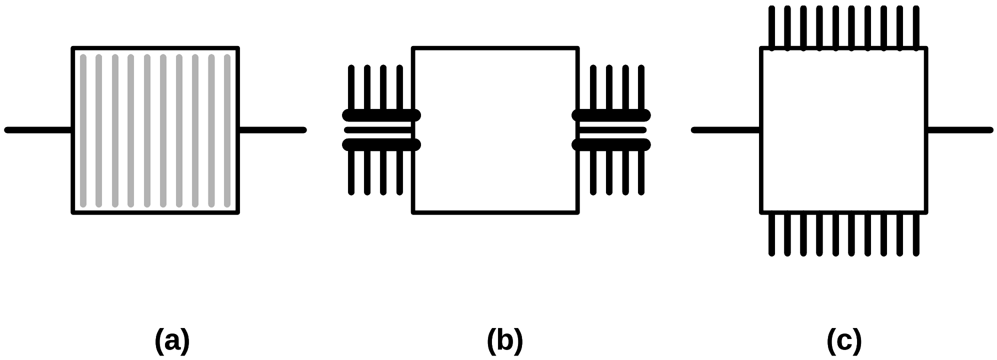

Fig. 5 Top views of various types of vertical combdrive-based scanners: (a) scanner with combs underneath the mirror; (b) scanner with comb integrated on a shaft parallel to the torsion bar; and (c) scanner with comb integrated at the edge of the mirror.

A large area 1.5 x 1.2 mm^2 scanning mirror with movable comb directly integrated underneath the mirror has been reported by Lee et al.,[44] The scanners were fabricated with DRIE and fixed and moving combs were fabricated in two separate SCS layers that were bonded together with a gold-tin layer utilizing a flip-chip aligner. The bottom silicon layer was anodically bonded to glass before the fixed combs were etched. The device achieved a 12° optical scan range with a 60 Hz sinusoidal signal at 28 V and a DC bias voltage of 35 V. The resonant frequency for the device was reported at 1.353 kHz. When fixed and moving combs are fabricated in separate layers, the alignment step is critical since it controls the electrode gap (5 μm in the reported device).

A scanning mirror with staggered vertical combdrive actuation was demonstrated by Conant et al.,[45] by patterning the fixed and moving teeth of the combdrive in two SCS layers separated by oxide (Fig. 6). The fixed teeth were patterned in the silicon substrate to a depth of 100 μm. The moving teeth were patterned in a 50 μm SCS layer created by fusion bonding after the substrate etch. Opened holes in the top silicon layer provided 0.2 μm alignment between the fixed and moving teeth. The device reported had very stiff torsion bars (50 μm thick x 15 μm wide x 150 μm) which resulted in an extremely high, 32 kHz resonant frequency for the 550 μm diameter mirror. The total optical scan angle in resonant mode was reported as 24.9° at 171 V_{rms}. For such a stiff device, resonant mode is required to achieve usable actuation at reasonable voltage, but the staggered vertical combdrive design is suitable for quasistatic actuation of more compliant torsion springs. Self-aligned vertical combdrives have been described by Krisnamoorthy and Solgaard [46,47], and are achieved by utilizing sacrificial comb teeth such that the final etch defines both the fixed and moving comb.

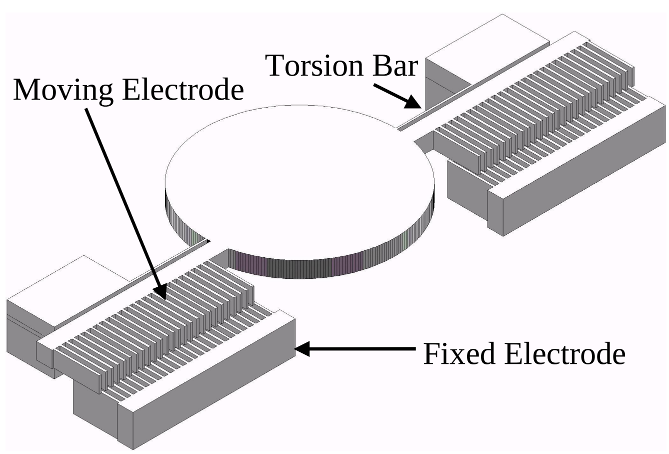

Fig. 6 Schematic of the staggered vertical combdrive actuated SCS scanner (after [45]).

At UCLA we have developed a truly self-aligned process with the angular vertical combdrive, AVC. [48] The self-aligned comb fingers are patterned in a single etch of the SOI layer. A polymer hinge is then applied to fasten the moving combs to the fixed combs and to provide the force for the surface tension assembly. [49] After release, heating of the polymer causes reflow which rotates the moving comb out of the wafer plane, upon cooling the thermoplastic polymer fastens the combs together at a fixed rotation angle (Fig. 7). This initial angle determines the maximum rotation angle for the device.[50] An AVC device (1 mm diameter) was demonstrated with a photoresist hinge derived from a 25 μm SOI layer. However, yield was low due to photoresist residue in the high aspect ratio features and the best static scan angle measured was 3.2° (mechanical range) at 108V for a scanner with a resonant frequency of 1.4 kHz. [51] We have recently reported a process utilizing benzocyclobutene (BCB), a negative photo-active material for the AVC. [52] The BCB process has yielded more AVC scanning devices and improved device performance has been measured on designs with more compliant springs. We have achieved a static scan angle of 14° (mechanical range) at 65 V, for a device with a resonant frequency of 598 Hz.[53] In addition to the SOI AVC device, we have developed a hybrid bulk-surface micromachined 2-D AVC.[54]

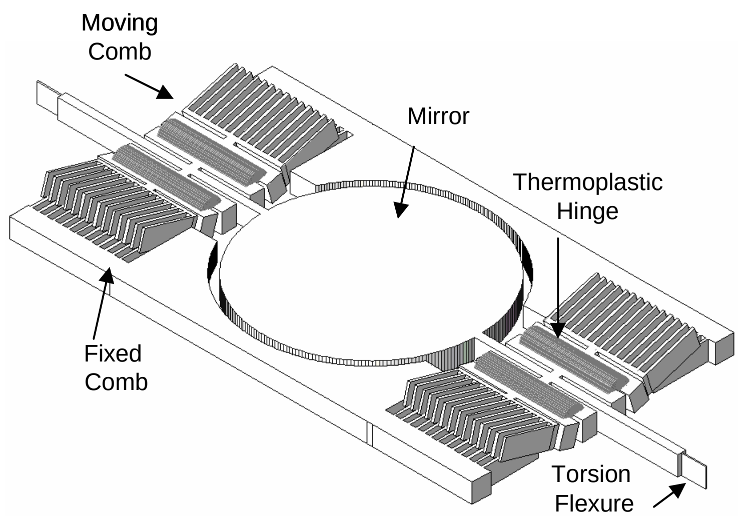

Fig. 7 Schematic of angular vertical comb (AVC) scanner.[53]

Scanners with self-assembled angular vertical combdrive actuators have also been reported by Xie et al. who employed stress-induced curling in a multilayered metal/oxide hinge to assemble the AVC [55] and Kim et al. who utilized plastic deformation to create an AVC. [56, 57] The silicon torsion bars were mechanically deformed while heating above the glass transition temperature, causing a permanent plastic deformation. Kim's device achieved a 50.9° optical scan range at the resonant frequency of 4.13 kHz at 30Vdc plus 14Vpp.

2-D vertical combdrive scanners are more difficult to implement than 2-D parallel plate type scanners since four isolated electric leads are needed for the fixed combs. This requires isolation schemes that allow the inner axis electrical path to crossover the outer axis to reach the terminal pads on top or connections from the bottom. A 2-D vertical combdrive scanner has been recently reported by Kwon et al., [58] which employs SOI and backside islands (insulated from the substrate by buried oxide) to achieve isolation of the inner and outer frames while maintaining mechanical continuity. The device was also designed for control of up and down i.e., piston motion.

Fujitsu has reported a 2-D vertical combdrive scanner with the comb fingers extended from the edge of the mirror.[59] Since the fingers are located at the edge where linear displacement is largest, much taller comb fingers are necessary to achieve the same scan range (100 μm in the reported device). The scanner was derived from a symmetric SOI wafer with both top and bottom silicon layers 100 μm thick separated by a 1 μm buried oxide. The top and bottom layers were differentially etched with DRIE and an oxide hard mask, so that thinned torsion bars and thinned electrical connection bars were possible in the top and bottom layers, respectively. The device achieves five electric potentials by electrically connecting to the four bottom isolated combs through gold bump bonds to another substrate with patterned electrodes.

The gold bumps also create a 120-μm gap to accommodate the mirror motion. The process was used to fabricate an 80 x 80 switch. The scan angle range was reported as 10° at 60 V under static conditions.

4. SCANNING MIRRORS WITH MAGNETIC AND ELECTROMAGNETIC ACTUATORS

As stated previously, magnetic actuation is practical when the mirror dimensions are on the millimeter scale since the magnetic torque (generated by the magnetic device interacting with an external magnetic field) scales with volume for permanent magnetic materials and with total coil area for electromagnets. (For an analysis of magnetic torque see Judy and Muller. [60]) In addition, the overall system size must accommodate the magnets (permanent or electric coils) used to generate the external magnetic field. Therefore, motivation for this type of scanner may be the price reduction afforded with batch fabrication techniques or lower power consumption rather than miniaturization per se. Miyajima et al. [61] point out that conventional optics use optical beams with spot sizes in the millimeter range and that relatively large area scanners are required if MEMS are to be integrated into such systems.

Magnetically actuated pop-up type scanning mirrors were demonstrated by Miller and Tai[62] utilizing bulk-silicon micromachining and by Judy and Muller[60] utilizing surface micromachining. In Miller and Tai's system, the scanning mirror was used to create and retrieve hundreds of stored holograms created by angle multiplexing. [61] The mirror angle was primarily controlled by the coil current of an external electromagnet. Micromirror devices with permalloy coatings only and with permalloy coatings plus patterned coils were demonstrated. The on-mirror copper patterned coils provided better angular resolution which improved the hologram spacing from 0.143° to 0.03° when compared to the mirrors with magnetic coating only. Both types of mirrors were approximately 4 x 4 mm^2 and achieved deflection angles of greater than 60° with response times ~ 30 msec.

Miyajima et al. at Olympus [63] have developed MEMS 1-D scanners (mirror size ~ 4.2 x 3.0 mm), for insertion into a commercial laser scanning confocal microscope. Their MEMS scanners were designed for fast or horizontal scanning in resonant mode at ~ 4 kHz. The scanners were fabricated from SOI wafers, essentially providing two SCS structural layers: the top silicon layer, used to define thinner torsion bars and the entire substrate thickness of 300 μm used to stiffen the mirror against deformation caused by residual stress and dynamic operation. (For analysis and discussion of dynamic deformation in MEMS scanners see Conant et. al [64] and Urey et. al [65]) A combination of DRIE and wet anisotropic etching was used for the top layer and the substrate, respectively. The mirror coils were formed from electroplated copper and sensing coils of sputtered aluminum were added to provide closed loop feedback for accurate mirror positioning. The authors reported that the device met or exceeded the requirements for the laser scanning confocal microscope application including stability and repeatability. In this application where the overall system is large (tabletop size), Olympus uses the MEMS scanner in conjunction with a macroscale scanner to achieve 2-D raster scanning. For smaller systems two electromagnetic MEMS mirrors may be cascaded [66] or with the tradeoff of design complexity, a single 2-D scanner may be used.

An early 2-D electromagnetic scanner demonstrated by Asada et al.,[67] was fabricated by bulk micromachining from a 200 μm thick silicon substrate with 16 μm thick electroplated copper coils. The inner plate (y-axis) was 4 x 4 mm^2 and the outer frame (x-axis) was 7 x 7 mm^2 with measured resonant frequencies of 1450 Hz and 380 Hz, respectively. Reported scan angles were low, even in resonant mode the scanner achieved less than 3 degrees for the x-axis and less than 1 degree for the y-axis at 35 mA coil current.

The current state of the art (as reported in the literature) shows improved performance for MEMS electromagnetic 2-D scanners. Ahn and Kim [68] have reported a SCS (70 μm thick substrate) scanner with layered thin films of BCB (benzocyclobutene), silicon nitride, and aluminum forming the torsion suspensions and serving as multi-level interconnect for independent control of the electromagnetic coils for the inner mirror and outer frame rotation axes. The mirror was 3.5 x 3.5 mm^2 and the outer frame was 5.7 x 5.7 mm^2 with measured resonant frequencies of 380 Hz and 150 Hz, respectively. The mirror inner coil currents must flow on the outer frame to reach the electrical terminals. To avoid crosstalk between the inner and outer axes, the mirror current was looped back through a parallel yet isolated path along the outer frame. Thus, a compensation current with equal magnitude yet opposite direction effectively cancelled the Lorenz force in these overlapping areas. Reported maximum scan angles (total optical scan range) were 5.44 degrees at 30 mA in resonance for the inner axis and 51.34 degrees at 130 mA in resonance for the outer axis.

An interesting approach for achieving remotely actuated 2-D scanner by magnetostrictive effect has been reported by Bourouina et al. [69,70]. In this work, 2-D scanning was achieved by simultaneously exciting two modes of motion, bending and twisting, in a cantilevered mirror. The scanner was fabricated from 20 μm SOI with a differential DRIE etch technique to obtain a thin compliant section through which the more rigid 100 μm mirror section attaches to a fixed frame. The device includes silicon piezoresistive sensors for feedback control, consisting of resistor bridges formed on the thin section with boron ion implantation into the n-type SOI. The backside of the device was sputter coated with a 4.5 μm magnetostrictive thin film of layered TbFe and CoFe developed for this application. The large devices (20 x 10 mm^2) were driven to bi-modal resonance by an external electromagnet with superimposed coil currents at 189 Hz and 1890 Hz, corresponding to the resonant frequencies for bending and torsion, respectively. Optical scan ranges for the modes were reported as 8.7 degrees for the horizontal axis (torsion) and 7.4 degrees for the vertical axis (bending).

A combined electrostatic/electromagnetic 2-D scanner has been developed by Microvision for retinal scanning displays. [64,71] These two-axis scanners utilize electromagnetic actuation for the outer frame that provides the vertical or slow axis, and electrostatic actuation for the inner mirror axis that provides the horizontal or fast axis. The devices were bulk micromachined utilizing both wet and dry anisotropic etching and electroplating was used to form electromagnetic coils on the outer frame. These scanners must be stiff to remain flat and withstand the forces developed in resonant scanning mode. The scanners also incorporated piezoresistive strain sensors on the torsion flexures for closed loop control. Scanner performance included 13.4° and 9.6° total mechanical scan range for the horizontal and vertical axes, respectively. The vertical axis drive signal (non-resonant mode) was at 60 Hz and the horizontal axis resonant mode drive signal was 19 kHz. The scanners are designed to meet SVGA video standards that require 800 x 600 resolution.

5. ALTERNATIVE ACTUATION METHODS

Besides the magnetic, electromagnetic, and electrostatic actuation discussed here, there have been scanners demonstrated with piezoelectric actuation [72,73,74] and thermal bimorph actuation [75,76].

6. CONCLUSION

We have described the design considerations with respect to actuator configuration and microfabrication for state of the art micromirror devices for 3-D optical switching and for imaging applications. The motivation toward single crystal silicon micromirrors through hybrid designs, and the adoption of combdrive actuators has been presented through the improved performance afforded as recorded in the literature.

ACKNOWLEDGEMENT

The authors would like to thank Drs. Lih Y. Lin and Li Fan for valuable discussions.

REFERENCES

1 Petersen, K.E., “Silicon as a Mechanical Material,” Proc. IEEE, vol. 70, no. 5, pp. 420-457, 1982.

2 Petersen, K. E., “Silicon torsional scanning mirror,” IBM J. R&D, vol. 24, pp.631-7, 1980.

3 M.C. Wu, "Micromachining for Optical and Optoelectronic Systems," Proc. IEEE, Vol. 85 (IEEE Press, Piscataway, N.J., 1997), pp. 1833–1856.

4 R.S. Muller and K.Y. Lau, “Surface-micromachined microoptical elements and Systems,” Proc. IEEE, Vol. 86, (IEEE Press, Piscataway, N.J., 1998), pp.1705-1720.

5 Ford, J.E., “OPTICAL MEMS: LEGACY OF THE TELECOM BOOM” 2004 Solid-State Sensor and Actuator Workshop Tech. Digest, June 6-10, Hilton Head, SC, pp.1-3.

6 M. Born and E. Wolf, *Principles of Optics*, 6th ed. Pergamon Press, 1980.

7 M.C. Wu and P.R.Patterson in *MEMS: A Practical Guide to Design, Analysis, and Applications*, eds., J.G. Korvink and O. Paul, Noyes Publications, in print, for fall 2004 publication.

8 Hagelin, P.M. and Solgaard, O., “Optical raster-scanning displays based on surface micromachined polysilicon mirrors,” IEEE J. Sel. Topics Quantum Elec., Vol. 5, p.67, 1999.

9 Degani, O., Socher, E., Lipson, A., Leitner, T., Setter, D. J., Kaldor, S., and Nemirovsky, Y., “Pull-In Study of an Electrostatic Torsion Microactuator,” IEEE J. Microelectromech. Syst., vol. 7, no. 4, pp. 373-379, 1998.
10 Hah, D., Toshiyoshi, H., and Wu, M.C., “Design of Electrostatic Actuators for MOEMS,” Proc. SPIE, Design, Test, Integration and Packaging of MEMS/MOEMS 2002, May 2002, Cannes, France
11 Multi-User MEMS Processes is offered by Cronos Microsystems, for details see http://www.memsrus.com/svcsmumps.html.
12 Fan, L., and Wu, M. C., "Two-Dimensional Optical Scanner with Large Angular Rotation Realized by Self-Assembled Micro-Elevator," Proc. IEEE LEOS Summer Topical Meeting on Optical MEMS, Paper WB4, August 20-22, 1998, Monterey, CA.
13 L. Fan, M. Wu, K. Choquette, and M. Crawford, "Self-assembled microactuated XYZ stages for optical scanning and alignment", International Conference on Solid-State Sensors and Actuators, (Transducers ’97), June 1997, Chicago, IL, pp. 319-322.
14 Aksyuk, V.A., Pardo, F., Bolle, C.A., Arney, S., Giles, C.R., Bishop, D.J., **“**Lucent Microstar micromirror array technology for large optical crossconnects,” Proceedings of the SPIE, MOEMS and Miniaturized Systems, Sept. 2000, Santa Clara, CA, pp. 320-324.
15 Aksyuk V.A., Simon, M.E., Pardo, F., Arney S., Lopez, D., and Villanueva, A., “Optical MEMS Design for Telecommunications Applications,” 2002 Solid-State Sensor and Actuator Workshop Tech. Digest, June 2-6, Hilton Head, SC, pp.1-6.
16 Neilson, D.T., et al.,“Fully Provisioned 112x112 Micro-Mechanical Optical Crossconnect With 35.8Tb/s Demonstrated Capacity,” Optical Fiber Communication Conference, OFC 2000, March 7-10, Baltimore, MD, Vol. 4, pp.202-204.
17 Lin, L.Y., Goldstein, E.L., “Opportunities and Challenges for MEMS in Lightwave Communications,” IEEE J. Sel. Topics Quantum Elec., Vol. 8, No. 1, p.163, 2002.
18 Syms, R.R.A., “Scaling Laws for MEMS Mirror-Rotation Optical Cross Connect Switches,” IEEE J. Lightwave Tech., Vol. 20, No. 7, p. 1084, 2002.
19 Kim, J., Papazian, A., Frahm, R.E., Gates, J.V., “Performance of Large Scale MEMS-Based Optical Crossconnect Switches,” IEEE/LEOS Conference 2002, Nov. 11-14, Glasgow, Scotland, UK, pp. 411-412.
20 Neilson, D.T. and Ryf, R. “Scalable Micro Mechanical Optical Crossconnects” IEEE/LEOS Conference 2000, Nov. 13-16, Rio Grande, Puerto Rico, Vol. 1, pp. 48-49.
21 Lin, H.-Y. and Fang, W., “Torsional Mirror with an Electrostatically Drive Lever-Mechanism,” Proc. IEEE/LEOS International Conference on Optical MEMS, Kauai, Hawaii, August 21-24, 2000. p.113-114.
22 Nee, J., Conat, R., Hart, M., Muller, R., and Lau, K., “Stretched-film micromirrors for improved optical flatness,” Proc. of IEEE MEMS 2000, Miyazaki, Japan, Jan. 23-27, 2000, pp. 704-709.
23 Drake, J. and Jerman,H., “A Micromachined Torsional Mirror for Track Following in Magneto-Optical Disk Drives”, 2000 Solid-State Sensor and Actuator Workshop, Hilton Head, SC, pp. 10-13.
24 G.-D. Su, H. Toshiyoshi, and M. C. Wu, “Surface-micromachined 2-D optical scanners with high-performance single-cystalline silicon micromirrors,” IEEE Photonics Technology Letters, Vol.13, pp. 606-608.
25 Guo-Dung J. Su, Pamela R. Patterson, and Ming C. Wu, “Surface-micromachined 2D optical scanners with optically flat single-crystalline silicon micromirrors,” Proc. of the SPIE - vol.4293, (Silicon-based and Hybrid Optoelectronics III, San Jose, CA, USA, 23-24 Jan. 2001, p.46-53.
26 P.Patterson, D. Hah, G.-D. Su, H. Toshiyoshi, and M.Wu, “MOEMS Electrostatic Scanning Micromirrors Design and Fabrication,” Integrated optoelectronics, proceedings of the first international symposium**,** eds., M.J. Deen, D. Misra, J. Ruzyllo, Pennington, NJ, Electrochemical Society, Inc.,2002, p.369.
27 U. Srinivasan, M. Helmbrecht, C. Rembe, R.S. Muller, and R.T. Howe, “Fluidic Self-Assembly of Micromirrors onto Surface Micromachined Actuators,” 2000 IEEE/LEOS International Conference on Optical MEMS, Kauai, HI, pp.59-60.
28 M. A. Michalicek and V. Bright “Flip-Chip fabrication of advanced micromirror arrays,” 14th IEEE International Conference on Micro Electro Mechanical Systems, (MEMS 2001), Interlaken, Switzerland, 21-25 Jan. 2001, pp.152-67.
29 Y.-A. Peter, E. Carter, and O. Solgaard, “Segmented Deformable Micro-Mirror for Free-Space Optical Communication,” 2002 IEEE/LEOS International Conference on Optical MEMS, Lugano, Switzerland, pp.197-198.
30 S. Blackstone and T. Brosnihan, “SOI MEMS Technologies for Optical Switching”, IEEE/LEOS International Conference on Optical MEMS, Sept. 25-28, 2001, Okinawa, Japan.
31 www.analog.com/library/analogDialogue/archives/36-04/mirrors/index.html
32 M.R. Dokmeci, S. Bakshi, M. Waelti, A. Pareek, C. Fung, and C.H. Mastrangelo, “Bulk Micromachined Electrostatic Beam Steering Micromirror Array,” 2002 IEEE/LEOS International Conference on Optical MEMS, Lugano, Switzerland, pp.15-16.
33 Sawada, R.; Yamaguchi, J.; Higurashi, E.; Shimizu, A.; Yamamoto, T.; Takeuchi, N.; Uenishi, Y. “Single Si crystal 1024ch MEMS mirror based on terraced electrodes and a high-aspect ratio torsion spring for 3-D cross-connect switch,” 2002 IEEE/LEOS International Conference on Optical MEMs, pp. 11 –12, 2002 Lugano, Switzerland.
34 Sawada, R.; Yamaguchi, J.; Higurashi, E.; Shimizu, A.; Yamamoto, T.; Takeuchi, N.; Uenishi, Y. “Improved Single Crystalline Mirror Actuated by Terraced Electrodes with High-Aspect Ratio Torsion Springs,” 2003 IEEE/LEOS International Conference on Optical MEMs, pp. 153 –154, 2003, Waikoloa, Hawaii.
35 Ryf, R., et al., “1296-port MEMS Transport Optical Crossconnect with 2.07 Petabit/s Switch Capacity,” Optical Fiber Communication Conference, OFC 2001, March 17-22, Anaheim, CA, Vol. 4, p. PD28-1.
36 V.A. Aksyuk, et al, “238x238 surface micromachined optical crossconnect with 2 dB maximum loss,” Optical Fiber Communications (OFC) Conference, Postdeadline paper, March 2002, Anaheim, CA.

37 J. Kim, A.R. Papazian, R.E. Frahm, and J.V. Gates, “Performance of large scale MEMS-based optical crossconnect switches,” 2002 IEEE/LEOS Annual Meeting, Paper WG-1, Glasgow, Scotland, November 10-14, 2002.
38 Tang, W.C., Nguyen, T.-C.H., Judy, M.W., Howe, R.T., “Electrostatic-comb drive of lateral polysilicon resonators,” Sensors and Actuators A (Physical), vol.A21, (no.1-3), 5th International Conference on Solid-State Sensors and Actuators and Eurosensors III, Montreux, Switzerland, 25-30 June 1989, p.328-31.
39 V. Milanovic, M. Last, K.S.J.Pister, “Torsional Micromirrors with Lateral Actuators” Transducers 01, Munich, Germany, pp.1290-1301.
40 Selvakumar, A.; Najafi, K.; Juan, W.H.; Pang, S. “Vertical comb array microactuators,” 8th IEEE International Conference on Micro Electro Mechanical Systems, (MEMS 1995), Amsterdam, Netherlands, pp. 43-8.
41 Selvakumar, A and Najafi, K., “Vertical Comb Array Microactuators,” IEEE J. Microelectromech. Syst., vol. 12, no. 4, pp. 440-449, 2003.
42 N. Yazdi, H. Sane, T.D. Kudrle, and C.H. Mastrangelo, “Robust Sliding-Mode Control of Electrostatic Torsional Micromirrors Beyond the Pull-In Limit,” International Conference on Solid-State Sensors and Actuators, (Transducers ’03), June 2003, Boston, MA, pp. 319-322.
43 H. Schenk, P.Dürr, T. Hasse, D. Kunze, U. Sobe, H.Kück, “Large Deflection Micromechanical Scanning Mirrors for Linear Scans and Pattern Generation”, IEEE Journal of Selected Topics in Quantum Electronics, vol. 6, no.5, Sept./Oct. 2000, pp.715-722.
44 J.-H. Lee; Y.-C. Ko; D.-H. Kong; J.-M. Kim; K.B. Lee; D.-Y. Jeon, “Design and fabrication of scanning mirror for laser display,” Sensors and Actuators A (Physical), vol.A96, no.2-3, pp.223-30, 2002.
45 R. A. Conant, J.T. Nee, K. Lau, R.S. Mueller “A Flat High-Frequency Scanning Micromirror”, 2000 Solid-State Sensor and Actuator Workshop, Hilton Head, SC, pp. 6-9.
46 U. Krisnamoorthy and O. Solgaard, “Self-aligned Vertical Comdrive Actuators for Optical Scanning Micromirrors” IEEE/LEOS International Conference on Optical MEMS, Sept. 25-28, 2001, Okinawa, Japan, p.41
47 U. Krisnamoorthy, D. Lee., O. Solgaard, “Self-aligned Vertical Electrostatic Combdrives for Micromirror Actuation” J. Microelectromech. Syst., vol. 12, no. 4, pp. 458-464, 2003.
48 P. R. Patterson, D. Hah, H. Chang, H. Toshiyoshi, M. C. Wu, “An Angular Vertical Comb Drive for Scanning Micromirrors”, IEEE/LEOS International Conference on Optical MEMS, Sept. 25-28, 2001, Okinawa, Japan, p.25
49 R.R.A. Syms, C. Gormley, S. Blackstone,"Improving Yield, Accuracy and Complexity in Surface Tension Self-Assembled MOEMS”, Sensors and Actuators A 88 (2001) 273-283.
50 D. Hah, P.R. Patterson, H.Nguyen, H. Toshiyoshi, and Ming C. Wu, “Theory and Experiments of Angular Vertical Comb-Drive Actuators for Scanning Micromirrors,” to be published in JSTQE (2004).
51 P. R. Patterson, D. Hah, H. Nguyen, R.-M. Chao, H. Toshiyoshi, Ming C. Wu, “A Scanning Micromirror with Angular Comb Drive Actuation,” The 15th IEEE International Micro Electro Mechanical Systems Conference (MEMS 2002), Jan. 20- 24, 2002, Las Vegas, NV.
52 H.Nguyen, D.Hah, P.R. Patterson, W. Piywattanametha,M.C.Wu, “A Novel MEMS Tunable Capacitor Based on Angular Vertical Comb Drive Actuators”, Solid-State Sensor & Actuator Workshop (Hilton Head 2002), June 2-6, 2002, Hilton Head Island, SC.
53 P. R. Patterson, “MEMS scanning micromirrors with a new electrostatic angular vertical combdrive,” PhD dissertation, University of California, Los Angeles, 2003.
54 W. Piyawattanametha, P. R. Patterson, D. Hah, H. Toshiyoshi, and M. C. Wu, “A Surface and Bulk Micromachined Angular Vertical Combdrive for Scanning Micromirrors,” in *Tech. Dig. Optical Fiber Conference (OFC 2003),* Atlanta, GA, USA, Mar. 23-28, 2003,
55 H. Xie, Y. Pan, and G. K. Fedder, “A CMOS-MEMS mirror with curled-hinge comb drives,” J. Microelectromech. Syst., vol. 12, pp. 450-457, Aug. 2003.
56 J. Kim, H. Choo, L. Lin, and R. S. Muller, “Microfabricated torsional actuator using self-aligned plastic deformation,” in Proc. Int. Conf. on Solid State Sensors, Actuators and Microsystems (Transducers ’03), Boston, MA, June 8-12, 2003, pp. 1015-1018.
57 J. Kim and L. Lin, “Batch-Fabricated Scanning Micromirrors Using Localized Plastic Deformation of Silicon,” 2004 Solid-State Sensor and Actuator Workshop Tech. Digest, June 6-10, Hilton Head, SC, pp.494-497.
58 S. Kwon, V. Milanovic, and L.P. Lee, “A high aspect ratio 2D gimbaled microscanner with large static rotation,” 2002 IEEE/LEOS International Conference on Optical MEMS, Lugano, Switzerland, pp.149-150.
59 Y.Mizuno, O.Tsuboi, N.Kouma, H.Soneda, H.Okuda, Y.Nakamura, S.Ueda, I.Sawaki, F.Yamagishi, “A 2-axis comb-driven micromirror array for 3D mems switches," 2002 IEEE/LEOS International Conference on Optical MEMS, Lugano, Switzerland, pp.153-154.
60 Judy, J.W. and Muller, R.S., “Magnetically Actuated, Addressable Microstructures,” IEEE J. Microelectromech. Syst., vol. 6, no. 3, pp. 249-256, 1997.
61 Miyajima, H., Asoaka, N., Arima, M., Minamoto, Y., Murakami, K., Tokuda, K., and Matsumoto, K., “A Durable, Shock-Resistant Electromagnetic Optical Scanner with Polyimide-Based Hinges,” IEEE J. Microelectromech. Syst., vol. 10, no. 3, pp. 418-424, 2001.
62 Miller, R., and Tai, Y.-C., “Electromagnetic MEMS Scanning Mirrors,” Optical Engineering, vol. 36, no. 5, pp. 1399-1407, May 1997.

63 Miyajima, H., Asoaka, N., Isokawa, T., Ogata, M., Aoki, Y., Imai, M., Fujimori, O., Katashiro, M., and Matsumoto, K., “Product Development of a MEMS Optical Scanner for a Laser Scanning Microscope,” The 15th IEEE International Micro Electro Mechanical Systems Conference (MEMS 2002), Jan. 20- 24, 2002, Las Vegas, NV. pp. 552-555.

64 Conant, R.A., Nee, J.T., Lau, K.Y., and Muller, R.S., “Dynamic Deformation of Scanning Mirrors,” 2000 IEEE/LEOS International Conference on Optical MEMS, Kauai,HI, pp.49-50.

65 Urey, H., Wine, D.W., and Osborn T.D., “Optical performance requirements for MEMS-scanner based microdisplays,” Proceedings of the SPIE, MOEMS and Miniaturized Systems, Sept. 2000, Santa Clara, CA. pp. 176-185.

66 Asada, N., Takeuchi, M., Vaganov, V., Belov, N., Hout, S., and Sluchak, I., “Silicon micro-optical scanner,” Sensors and Actuators, A, Physical, vol. 83, pp. 284-290, 2000.

67 Asada, N., Matsuki, H., Minami, K., and Esashi, M., “Silicon Micromachined Two-Dimensional Galvano Optical Scanner,” IEEE Trans. on Magnetics, vol. 30, no. 6, pp. 4647-4649, 1994.

68 Ahn, S.-H., Kim, Y.-Y., “Galvanometric silicon scanning mirror with 2 DOF,” 2002 IEEE/LEOS International Conference on Optical MEMS, Lugano, Switzerland, pp.87-88.

69 Garnier, A., Bourouinna, T., Fujita, H., Orsier, E., Masuzawa, T., Hiramoto, T., Peuzin, J.-C., “A Fast, Robust and Simple 2-D Micro-Optical Scanner Based on Contactless Magnetostrictive Actuation,” The 13th IEEE International Micro Electro Mechanical Systems Conference (MEMS 2000), Jan. 2000, Miyazaki, Japan, pp. 715-720.

70 Bourouina,T., Lebrasseur,E., Reyne,G., Debray,A., Fujita, H., Ludwig, A., Quandt, E., Muro, H., Oki, T., and Asaoka, A., “Integration of Two Degree-of-Freedom Magnetostrictive Actuatio and Piezoresistive Detection: Application to a Two-Dimensional Optical Scanner,” IEEE J. Microelectromech. Syst., vol. 11, no. 4, pp. 355-361, 2002.

71 D.W.Wine, M.P. Helsel, L.Jenkins, H. Urey and T.D. Osborn, “Performance of a Biaxial MEMS-Based Scanner for Microdisplay Applications,” Proceedings of the SPIE, MOEMS and Miniaturized Systems, Sept. 2000, Santa Clara, CA. pp. 186-196.

72 Yamada, K., Kuriyama, T. **“**A novel asymmetric silicon micro-mirror for optical beam scanning display,” IEEE Eleventh Annual International Workshop on Micro Electro Mechanical (MEMS 98), 25-29 Jan. 1998, Heidelberg, Germany, pp.110-15.

73 H.-J. Nam, Y.-S. Kim, S.-M. Cho, Y. Yee, and J.-U. Bu, “Low Voltage PZT Actuated Tilting Micromirror with Hinge Structure,” 2002 IEEE/LEOS International Conference on Optical MEMS, Lugano, Switzerland, pp.89-90.

74 J. Tsuar, L. Zhang, R. Maeda, S. Matsumoto, “2D Micro Scanner Actuated by Sol-gel Derived Double Layered PZT,” Fifteenth IEEE International Conference on Micro Electro Mechanical Systems (MEMS 2002) Fifteenth IEEE 20-24 Jan. 2002, Las Vegas, NV, pp.548-551.

75 Sinclair, M. A “High frequency resonant scanner using thermal actuation,” Fifteenth IEEE International Conference on Micro Electro Mechanical Systems (MEMS 2002) Fifteenth IEEE 20-24 Jan. 2002, Las Vegas, NV, pp.698-701.

76 H. Xie, Y. Pan, and G. Fedder, “A SCS CMOS Micromirror for Optical Coherence Tomographic Imaging,” Fifteenth IEEE International Conference on Micro Electro Mechanical Systems (MEMS 2002) Fifteenth IEEE 20-24 Jan. 2002, Las Vegas, NV, pp.495-498.